23rd International Conference on Renewable Energies and Power Quality (ICREPQ'25)
Tenerife (Spain), 25th to 27th June 2025
ISBN-13: 978-84-09-66511-2

Analysis of Phase Comparison Application in Power Transformer Protection Against Internal Faults

J. Krstivojević[1], P. Eguia[2], M. Djuric[1], D.M. Larruskain[2], E.Torres[2]
[1] Department of Power Systems
University of Belgrade - School of Electrical Engineering, 11000 Belgrade, Serbia
e-mail: j.krstivojevic@etf.rs

[2] Department of Electrical Engineering
EIB University of the Basque Country UPV/EHU
Plaza Ingeniero Torres Quevedo 1, 48013 Bilbao (Spain)
e-mail: pablo.eguia@ehu.eus

Abstract. This paper investigates the application of phase comparison between primary and secondary currents for detecting internal short circuits in power transformers. The directional index, derived from a digital phase comparator, is used as an indicator of the phase shift between these currents. A methodology for internal fault detection is proposed, based on two sequential conditions: an identification phase triggered by an overcurrent condition and a directional index assessment for the fault decision phase. The methodology is tested using MATLAB/Simulink generated signals, where inter-turn faults affecting different percentages of transformer windings are simulated. The proposed approach is compared with conventional differential protection in terms of sensitivity and operating speed. The paper presents the algorithm and the results of the conducted tests.

Key words. power transformer, internal fault detection, inter-turn faults, phase comparison, relay protection.

1. Introduction

Effective protection of power transformers (PT) is crucial for the stable and secure operation of the power system [1]. Power transformer protection schemes vary based on application, importance, and cost-effectiveness. To minimize damage from thermal and electromechanical stress, disconnection from the network should occur at the earliest possible moment after a fault [2]. Differential protection is the most common type of protection for PTs above 10 MVA, serving as the primary protection against internal faults [1]. This protection protects PT from inter-turn short circuits, phase-to-phase short circuits, and phase to ground short circuits if the transformer star point is directly grounded [1,3]. If the PT star point is grounded through active resistance or low-impedance, ground fault protection is used as a sensitive protection against single-phase to ground short circuits [1].

Differential protection calculates the differential and restraint currents and, based on their values, takes appropriate action. While differential protection demonstrates high reliability in detecting severe internal faults, its sensitivity may be limited in cases where the percentage of short-circuited windings is small or when fault currents are low, such as ground faults close to the transformer neutral point (turn-to-ground faults) [4]. Between 70% and 80% of transformer failures are attributed to internal winding insulation failure [5]. Gradual insulation degradation, partial discharges, and exposure to thermal stress, moisture or bubbles often trigger these faults, which typically begin with a small percentage of winding turns and worsen over time [6]. This way, inter-turn faults can escalate into severe ground faults involving the transformer core or cause extensive arcing within the tank, resulting in significant damage. Early detection and prompt disconnection from the grid can prevent fault progression, enabling cost-effective repairs and minimal downtime [7]. However, conventional differential relays, commonly used for PT protection, struggle to detect incipient inter-turn faults, requiring at least 10% of the winding to be involved for reliable detection [1]. Consequently, identifying early-stage inter-turn faults remains a significant challenge in transformer protection [6,8].

In recent years, several methods and new approaches have been applied to improve differential protection, including the time domain differential protection scheme [9], using the Teager Energy Operator and a fluctuation identifier index [10], the application of the discrete energy separation algorithm [11], support vector machine and wavelet transform [12], and the integral principle, where the required criteria signals are calculated directly from the operational and restraining currents [13].

The objective of this paper is to examine the possibility of applying phase comparison of primary and secondary currents for protection against internal short circuits. In this paper, the digital phase comparator presented in [14] will be used. The application of the directional index, which represents a normalized value of the digital phase comparator, has been proposed in [15]. This index has been successfully applied for PT ground fault protection, as well as in an algorithm for detecting external short circuits [16], where it serves as an additional criterion for differential protection by blocking it during external faults accompanied by current transformer saturation.

Since the directional index has demonstrated good characteristics in terms of speed and convergence, this paper investigates its applicability for detecting internal short circuits. A new methodology based on the directional index is proposed, with an emphasis on its potential for internal fault detection. The study also examines the variation of the directional index depending on the percentage of short-circuited transformer winding turns, as well as on the position of the power transformer within the network. The proposed methodology is compared with conventional differential protection. The results show that, in all analyzed cases, the algorithm based on the proposed methodology successfully identified internal faults and activated the trip signal faster than the conventional differential protection.

2. Theoretical Framework

A. The digital phase comparator

The digital phase comparator applied in this paper operates by calculating the integral of the product of current signals over an interval corresponding to half of the fundamental period [14-16]. Its normalized value is obtained by dividing this integral by the RMS indicators of the current signals, which are also calculated over the half of the fundamental period. This normalization provides directional index that serves as an indicator of the phase shift between the two current signals. Consequently, digital phase comparison of i_1 and i_2 is performed using expression (1).

$$Directional\ index = \frac{\frac{2}{m}\sum_{n=1}^{m/2} i_1(n)\cdot i_2(n)}{I_{\mathrm{RMS1}}\cdot I_{\mathrm{RMS2}}} \tag{1}$$

where: m is the number of samples in the fundamental period of the signal, $i_1(n)$ is the n-th sample of the current i_1, $i_2(n)$ is the n-th sample of the current i_2, I_{RMS1} and I_{RMS2} are RMS indicator values of the currents i_1 and i_2, calculated using the following expression:

$$I_{RMS} = \sqrt{\frac{2}{m}\sum_{n=1}^{m/2} i(n)\cdot i(n)} \tag{2}$$

When currents i_1 and i_2 are periodic, the directional index represents the cosine of the phase shift angle between them. If currents i_1 and i_2 are in phase, the directional index equals 1, whereas for currents in counter phase, with a phase shift of 180°, the directional index is -1.

B. Directional Index in Power Transformer Protection

A three-phase transformer with arbitrary winding connections and hourly index, for which phase compensation has been applied for the phase angle shift between the primary and secondary currents, is analyzed. During normal operating conditions and faults outside the protected zone of the PT, the phase shift (φ) between the primary and secondary currents is approximately 0° (Fig. 1), while during short circuits on the PT winding, the phase shift (φ) is greater than 0°. Depending on the PT's position in the system, the analysis of phase shift variation (φ) during short circuits on the PT winding considers two distinct cases. When the PT is positioned between two active networks, the phase shift (φ) varies within the range of 0° to 180°, whereas during short circuits on the PT winding located between an active network and a load, the phase shift (φ) remains within the range of 0° to 90°. Accordingly, the directional index is equal to 1 under normal operating conditions and for faults outside the protected zone, whereas during internal faults, it takes values within the range of: $-1 \le Directional\ index < 1$.

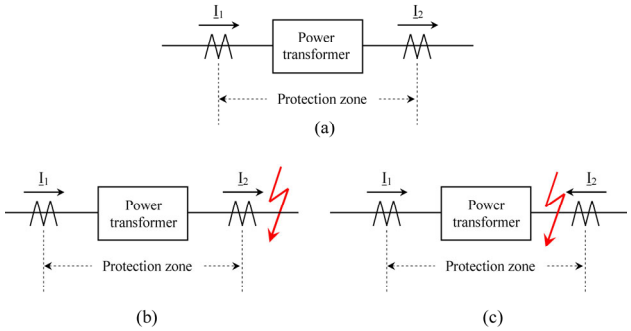

Fig. 1. Current directions during (a) normal operating conditions, (b) external short circuit, and (c) internal short circuit.

It should be noted that for a 100% short circuit of the PT winding positioned between an active and a passive network, the current on the passive network side is equal to zero. However, during the initial stage of such a fault, the directional index value and RMS indicators (calculated over half a period) do not immediately drop to zero and persist for a period of time long enough for the protection algorithm to make a proper decision.

3. Methodology

A. The simulation model

The signals used to test the proposed methodology were generated through computer simulations in MATLAB/Simulink. The simulation model corresponds to the scheme in Fig. 2. The element parameters applied in the simulation model are as follows. Network 220 kV: three-phase short-circuit level at the base voltage S_{sc1}=2000 MVA, ratio X/R = 14; Network 132 kV: S_{sc2}=2000 MVA, X/R = 7; Three-phase two winding PT: 220 kV/132 kV, 225 MVA, having YGyg0 connected windings, r_t = 0.0032 pu, x_t = 0.15 pu. The PT model has been developed to include internal faults and is based on the representation of a magnetic core coupled to two sets of three-phase coils. This model provides the option to specify the percentage of short-circuited turns in phase C on the secondary winding of the PT. The signals obtained from simulations are used to analyze the variation of the directional index for different percentages of inter-turn faults.

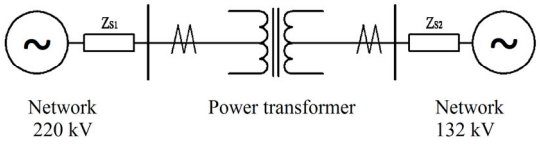

Fig. 2. The simulation model scheme.

B. Decaying DC component filter

To eliminate the DC component from input signals, the filter forms an auxiliary signal by subtracting the previous signal sample from the current one (3) [17].

$$s_f(k) = s(k) - s(k-1), \quad (3)$$

where: $s_f(k)$ represents the k-th sample of the filtered signal; $s(k)$ denotes the k-th sample of the input signal at time t; $s(k\text{-}1)$ refers to the $(k\text{-}1)$-th sample taken at time $(t\text{-}T_s)$; and T_s is the sampling interval, defined as $T_s = T/m$.

This DC filter effectively reduces the level of the decaying DC component in the input signals while introducing only a one-sample delay. It also produces a positive phase shift in the auxiliary signal, which increases with the sampling rate m. Since all input signals are processed through the same filter, this phase shift between the input and auxiliary signals does not affect the operation of the phase comparison.

The amplitude of the fundamental harmonic in the auxiliary signal s_f is also influenced by the number of samples m. Equation (4) defines the relationship between the fundamental harmonic amplitudes of the original signal s and the filtered signal s_f.

$$\frac{|\underline{S}_1|}{|\underline{S}_f|} = \frac{1}{2 \cdot \sin(\pi/m)}. \quad (4)$$

C. The algorithm

The algorithm is performed through the following steps.

Step 1: The initial step consists of performing magnitude and phase matching. In the case of a three-phase two-winding PT with an arbitrary winding connection, the currents on the primary and secondary sides of the PT must undergo magnitude and phase matching. The algorithm steps described below refer to one pair of the currents from the PT primary and secondary sides for which magnitude and phase matching has been performed.

Step 2: A decaying DC component filter is applied to compensate for the presence of a decaying DC component in the primary and secondary current signals.

Step 3: Calculation of the primary and secondary RMS indicators (I_1 and I_2) and the directional index.

Step 4: The first condition requires that either the primary or secondary RMS indicator exceeds a predefined value (I_{th}). By introducing an overcurrent condition, the *identification phase* is initiated.

$$I_1 > I_{th} \vee I_2 > I_{th} \quad (5)$$

If this condition is met, the next step is executed; otherwise, the algorithm returns to the beginning.

Step 5: The next condition represents the *fault discrimination phase* and verifies whether the directional index falls below the predefined threshold (6). If this condition is satisfied, it confirms the presence of a significant phase shift between the primary and secondary currents, indicating that the fault is within the protected zone.

$$Directional\ index < Directional\ index_{th} \quad (6)$$

Step 6: This step represents the *tripping decision*. The tripping signal will be activated if conditions (5) and (6) are met.

The elimination of unnecessary operation during the energization of an unloaded PT and PT overexcitation is achieved by restraint due to the presence of higher harmonics, as in conventional differential protection.

D. Testing the algorithm

The paper compares the performance of the algorithm based on the proposed methodology and the conventional differential protection algorithm in terms of sensitivity and operating speed.

Settings for the percentage differential protection with dual slope tripping characteristic: horizontal segment of the characteristic for $I_{d,min}$=0.3 p.u; restraint current at first break point $I_{r,1}$=1 p.u., and slope m_1=0.2; restraint current at second break point $I_{r,2}$=5 p.u, and slope m_1=0.5. The differential and restraint currents are obtained based on the following equations:

$$I_d = |\underline{I}_1 - \underline{I}_2|, \quad (7)$$

$$I_r = 0.5 \cdot |\underline{I}_1 + \underline{I}_2|. \quad (8)$$

Settings for the algorithm based on the proposed methodology are: I_{th}=1.15I_{nom}, where I_{nom} is nominal transformer current, and *Directional index*$_{th}$=0.95.

The selection of the directional index threshold is based on the minimum pickup current, set to $I_{d,min}$ = 0.3 p.u, under the assumption that the primary current (I_1) equals 1 p.u. The maximum phase shift between the primary and secondary (I_2) currents is calculated to be φ = 17.458°, occurring at a secondary current of 0.95 p.u. Based on this, the maximum threshold value of the directional index is:

$$Directional\ index_{th\_max} = \cos(\varphi) = 0.954, \quad (9)$$

and the setting *Directional index*$_{th}$=0.95 is selected to ensure a safety margin below the calculated maximum.

4. Simulation results

In the simulations conducted in this paper, the number of samples per cycle is 40, with the fault inception time corresponding to the 80th sample.

A. PT positioned between two active networks

The simulation results for the PT positioned between two active networks are presented below. Fig. 3 and Fig. 4 show the results for the 10% inter-turn fault case, while Fig. 5 and Fig. 6 correspond to the 50% inter-turn fault case. As can be seen in the figures, in both presented cases, the proposed algorithm effectively detected the presence of an internal fault and activated the trip signal before the percentage differential protection algorithm.

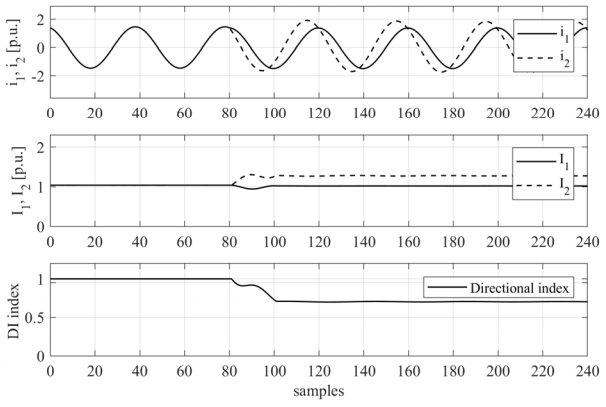

Fig. 3. 10% Inter-turn fault case: current waveforms, RMS indicators, and directional index.

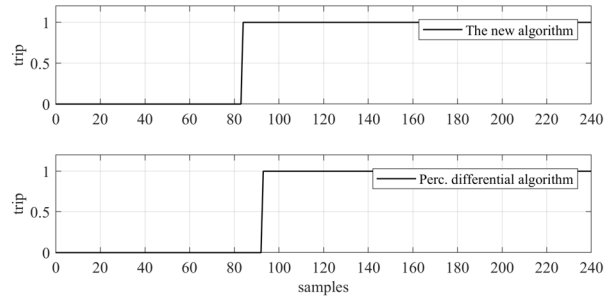

Fig. 4. 10% Inter-turn fault case: trip decisions using the new method and percentage differential protection algorithms.

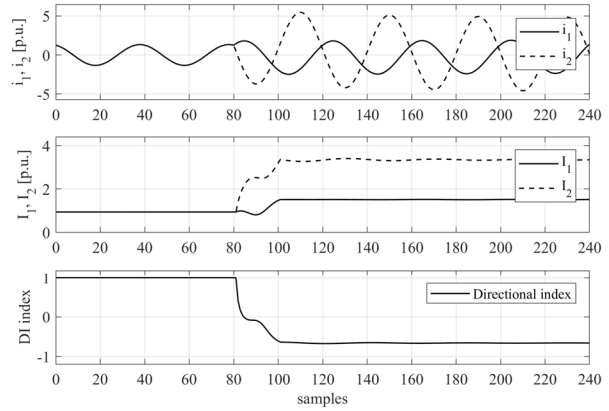

Fig. 5. 50% Inter-turn fault case: current waveforms, RMS indicators, and directional index.

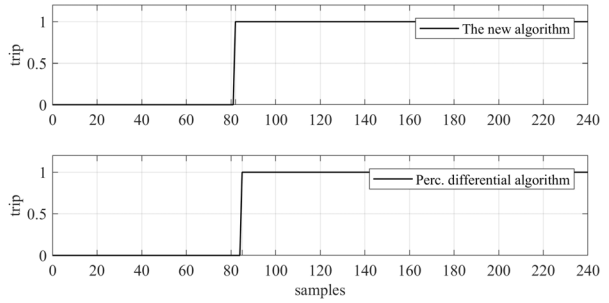

Fig. 6. 50% Inter-turn fault case: trip decisions using the new method and percentage differential protection algorithms.

The values of the directional index corresponding to different percentages of short-circuited turns in the transformer winding are shown in Table I. The table presents the results for 10%, 20%, 30%, 50%, and 90% of short-circuited turns. The index value is read 21 samples after fault inception, accounting for the fact that the directional index is calculated over a signal half-period (20 samples), and with one additional sample delay introduced by the DC filter.

Table I. - Directional index for PT positioned between two active networks

Percentage of inter-turn fault	10%	20%	30%	50%	90%
Directional index	0.708	0.23	-0.147	-0.641	-0.882

The activation times of the trip signal for both the proposed algorithm and the percentage differential algorithm are presented in Table II, expressed in number of samples measured from the moment of fault inception.

It can be observed that, in all analyzed cases, the proposed algorithm identified the fault faster than the percentage differential protection algorithm.

The results show that the directional index exceeded the set threshold 3 samples after fault inception in the case of a 10% inter-turn fault, whereas for all other analyzed cases, the threshold was crossed 2 samples after the short-circuit occurred. In the same 10% inter-turn fault scenario, the RMS indicator reached its predefined threshold 4 samples after fault inception, while in all other observed cases, the threshold was exceeded after 2 samples.

Table II. - Activation of trip signals for PT positioned between two active networks

Percentage of inter-turn fault	10%	20%	30%	50%	90%
The new algorithm [samples]	4	2	2	2	2
Perc. differential algorithm [samples]	13	8	7	5	4

B. PT positioned between the active and passive networks

To evaluate the algorithm's performance when the PT is positioned between the active and passive networks, the 132 kV side in the simulation model is represented by a passive load. Fig. 7 and Fig. 8 show the results for the 10% inter-turn fault case, while Fig. 9 and Fig. 10 correspond to the 50% inter-turn fault case, for the scenario in which the PT is positioned between the active and passive networks. In both cases, the proposed algorithm detected the internal fault and initiated the trip signal before the percentage differential protection algorithm.

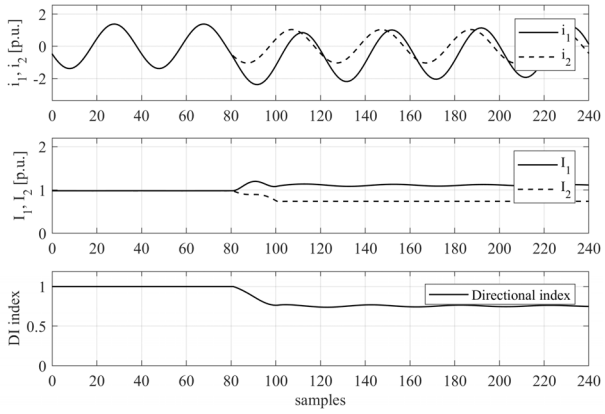

Fig. 7. 10% Interturn fault case: current waveforms, RMS indicators, and directional index, for PT positioned between the active and passive networks

Table III presents the directional index values for various percentages of short-circuited turns in the transformer winding, in the case where the PT is positioned between the active and passive networks. The values are read 21 samples after fault inception (as explained in the description of Table I). Table IV shows the trip signal activation times, given in samples from fault inception, for the case in which the PT is located between the active and passive networks. The results demonstrate that, in all considered fault cases, the proposed algorithm activates

the trip signal before the percentage differential protection algorithm.

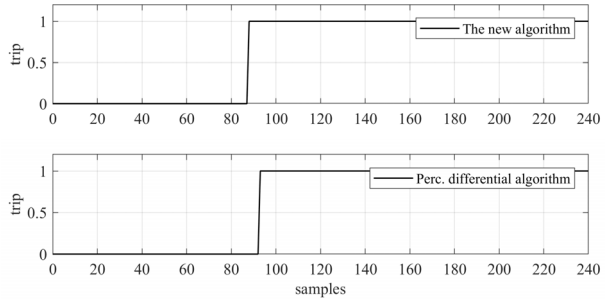

Fig. 8. 10% Interturn fault case: trip decisions using the new method and percentage differential protection algorithms, for PT positioned between the active and passive networks

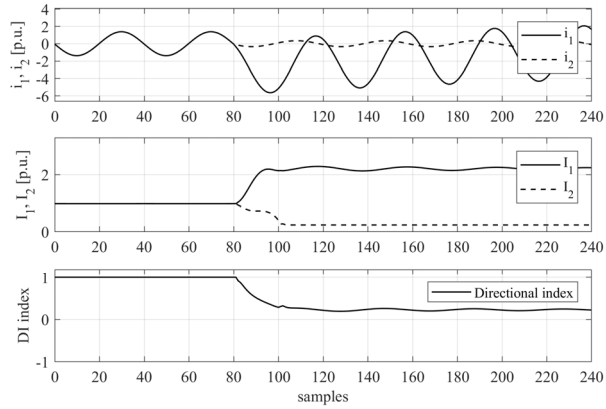

Fig. 9. 50% Interturn fault case: current waveforms, RMS indicators, and directional index, for PT positioned between the active and passive networks

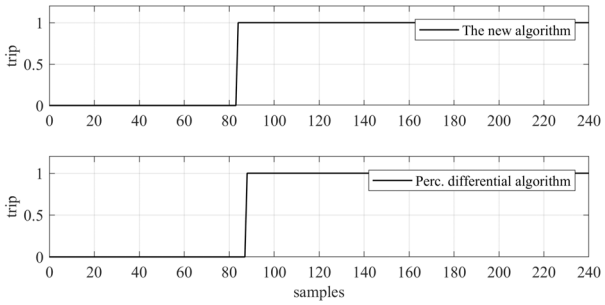

Fig. 10. 50% Interturn fault case: trip decisions using the new method and percentage differential protection algorithms, for PT positioned between the active and passive networks

Table III. - Directional index for PT positioned between the active and passive networks

Percentage of inter-turn fault	10%	20%	30%	50%	90%
Directional index	0.767	0.509	0.354	0.3	0.16

Table IV. - Activation of trip signals for PT positioned between the active and passive networks

Percentage of inter-turn fault	10%	20%	30%	50%	90%
The new algorithm [samples]	8	5	4	4	2
Perc. differential algorithm [samples]	13	10	8	6	6

Fig. 11 presents the results for an external short circuit. The figure shows that the directional index remains equal to 1 p.u. both before and after the short circuit occurs.

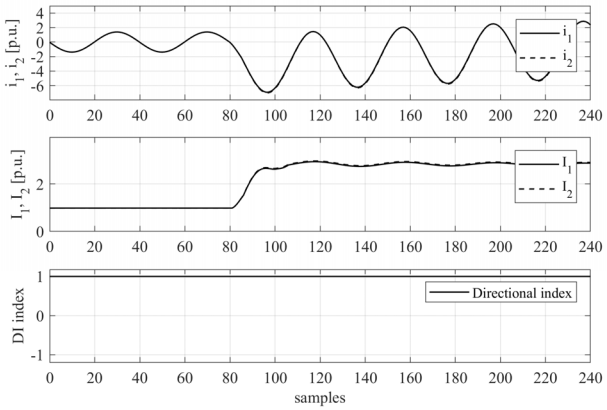

Fig. 11. External fault: current waveforms, RMS indicators, and directional index

The aim of this paper is to analyze the application of the phase comparison principle in power transformer protection against internal faults. The effect of current transformer (CT) saturation during external faults has not been taken into account. To prevent unnecessary operation during external faults, an additional algorithm could be used to detect faults outside the protection zone and to generate a blocking signal before CT saturation occurred, as suggested in [16].

As an extension to the proposed algorithm, a higher harmonic restraint function is assumed in order to eliminate unwanted operation during the energization of an unloaded PT and in cases of PT overexcitation. As shown in [18], restraint due to the presence of higher harmonics also eliminates unnecessary tripping during external faults involving CT saturation.

The presented results indicate that the application of phase comparison enables effective detection of an internal short circuit. In the identification phase of the algorithm, an overcurrent function is used to monitor whether the current in either the primary or secondary winding exceeds a predefined threshold.

As an additional variation of the phase comparison-based algorithm, instead of the overcurrent function and condition (5), Step 4 of the proposed algorithm can be modified so that the identification phase is based on the observation of the primary and secondary superimposed currents (9) and (10). The superimposed current is calculated by subtracting the current sample from the corresponding sample one cycle earlier. When any of the specified conditions, (9) or (10), is met, the algorithm proceeds to Step 5. To improve protection security, the transition to the next step can be allowed only after condition (9) or (10) has been satisfied in three consecutive evaluations.

$$\left|i_1(k) - i_1(k-m)\right| > \Delta i_{th} \tag{9}$$

$$\left|i_2(k) - i_2(k-m)\right| > \Delta i_{th} \tag{10}$$

Table V shows the activation of trip signals when the identification phase is based on superimposed currents, with Δi_{th} = 0.1 p.u. It can be observed that, in this case as

well, by using the modified Step 4 of the algorithm, the internal fault was effectively detected in all analyzed cases.

Table V. - Activation of trip signals when the identification phase is based on superimposed currents

Percentage of inter-turn fault	10%	20%	30%	50%	90%
PT betw. two active networks [samples]	4	4	4	4	4
PT betw. the active and passive networks [samples]	8	5	4	4	4

The application of the phase comparison-based algorithm has proven to be effective for detecting internal faults in PTs. Future work will focus on validating the proposed algorithm using real signals recorded in the field by protection relays. In addition, the algorithm will be implemented and tested in a Hardware-in-the-Loop (HIL) environment to evaluate its performance under more realistic conditions and to ensure its applicability in practice.

5. Conclusion

The paper presents a methodology for internal fault detection in power transformers, based on phase comparison between primary and secondary currents using a directional index. The algorithm includes two main steps: identification and fault discrimination. The results confirm that the proposed approach can reliably detect internal faults. The use of the directional index proved to be fast, stable, and effective, which makes it a promising option for further development and possible integration into protection systems.

Acknowledgement

The authors would like to thank the European Union's HORIZON WIDERA-2021-ACCESS-03 project SUNRISE, under grant agreement No. 101079200, for its financial support of this research. Also, the first author acknowledges that this work was financially supported by the Ministry of Science, Technological Development and Innovation of the Republic of Serbia under contract number: 451-03-137/2025-03/200103.

References

[1] IEEE Guide for Protecting Power Transformers, IEEE Std. 37.91, 2021.

[2] M. Dashtdar, D. Rahman, R.S. Hamid, "Distribution network fault section identification and fault location using artificial neural network" in 5th International conference on electrical and electronic engineering (ICEEE), 2018, pp. 273–278.

[3] A. Guzmán, S. Zocholl, G. Benmouyal, . H. J. Altuve, "A Current-Based Solution for Transformer Differential Protection - Part I: Problem Statement," IEEE Trans. Power Delivery, Vol. 16, No. 4, pp. 485-491 Oct. 2001.

[4] M.N.O. Aires, R.P. Medeiros, F.B. Costa, K.M. Silva, J.J. Chavez, M. Popov, "A wavelet-based restricted earth-fault power transformer differential protection," Electric Power Systems Research, Volu. 196, 2021, 107246, ISSN 0378-7796, https://doi.org/10.1016/j.epsr.2021.107246.

[5] N. Farzin, M. Vakilian, E. Hajipour, "Transformer turn-to-turn fault protection based on fault-related incremental currents," IEEE Trans. Power Delivery, vol. 34, no. 2, pp. 700–709, Apr. 2019.

[6] S. A. Ahmadi, M. Sanaye-Pasand, M. Abedini, M. H. Samimi, "Online Sensitive Turn-to-Turn Fault Detection in Power Transformers," IEEE Trans. Industrial Electronics, vol. 69, no. 12, pp. 13555-13564, Dec. 2022, doi: 10.1109/TIE.2022.3140504.

[7] L. M. R. Oliveira. A. J. M. Cardoso, "A Permeance-based transformer model and its application to winding interturn arcing fault studies," IEEE Trans. Power Delivery, vol. 25, no. 3, pp. 1589–1598, Jul. 2010.

[8] L. Oliveira, A. Cardoso, "Comparing power transformer turn-to-turn faults protection methods: negative sequence component versus space-vector algorithms", IEEE Trans. Industry Application, vol. 53, no. 3, 2017, pp. 2817–2825.

[9] Z. Moravej, A. Ebrahimi, M. Pazoki, M. Barati, "Time domain differential protection scheme applied to power transformers", International Journal of Electrical Power & Energy Systems, Volume 154, 2023, 109465, ISSN 0142-0615, https://doi.org/10.1016/j.ijepes.2023.109465.

[10] S. Hasheminejad, "A new protection method for the power transformers using Teager energy operator and a fluctuation identifier index", Electric Power Systems Research, Volume 213, 2022, 108776, ISSN 0378-7796, ttps://doi.org/10.1016/j.epsr.2022.108776.

[11] S. M. L. Moosavi, Y. Damchi, M. Assili, "A new fast method for improvement of power transformer differential protection based on discrete energy separation algorithm", International Journal of Electrical Power & Energy Systems, Volume 136, 2022, 107759, ISSN 0142-0615, https://doi.org/10.1016/j.ijepes.2021.107759.

[12] L. D. Simões, H. J. D. Costa, M. N. O. Aires, R. P. Medeiros, F. B. Costa, A. S. Bretas, "A power transformer differential protection based on support vector machine and wavelet transform", Electric Power Systems Research, Volume 197, 2021, 107297, ISSN 0378-7796, ttps://doi.org/10.1016/j.epsr.2021.107297.

[13] D. Bejmert, M. Kereit, F. Mieske, W. Rebizant, K. Solak, A. Wiszniewski, "Power transformer differential protection with integral approach", International Journal of Electrical Power & Energy Systems, Volume 118, 2020, 105859, ISSN 0142-0615, https://doi.org/10.1016/j.ijepes.2020.105859.

[14] Z. Stojanović, M. Djurić, "The algorithm for directional element without dead tripping zone based on digital phase comparator", Electric Power Systems Research, 81, 2011, pp. 377–383.

[15] J. Krstivojevic, M. Djurić, "A New Method of Improving Transformer Restricted Earth Fault Protection", Advances in Electrical and Computer Engineering, vol. 14; no. 3: pp. 41-48, 2014.

[16] J. Krstivojevic, M. Djuric, "A new algorithm for avoiding maloperation of transformer differential protection", The 10th Mediterranean Conference on Power Generation, Transmission, Distribution and Energy Conversion (MedPower 2016), Belgrade, Serbia, Nov. 2016, pp. 1-6.

[17] J. L. Domínguez, J. F. M. Argüelles, M. Angel, Z. Arrieta, B. L. Jaurrieta, M. S. Benito, I. A. Zugazaga, "New quick-convergence invariant digital filter for phasor estimation", Electric Power Systems Research Vol.79 (No.5), pp. 705–713. 2009.

[18] M. Stanbury, Z. Djekic, "The Impact of Current-Transformer Saturation on Transformer Differential Protection," IEEE Trans. Power Delivery, vol. 30, no. 3, pp. 1278-1287, June 2015, doi: 10.1109/TPWRD.2014.2372794.